

The Journey of the Lunar Flashlight Propulsion System from Launch through End of Mission

Celeste Smith, Nathan Cheek
Jet Propulsion Laboratory, California Institute of Technology
4800 Oak Grove Drive, Pasadena, CA 91109; (818) 354-4321
celeste.r.smith@jpl.nasa.gov nathan.cheek@jpl.nasa.gov

Christopher Burnside
NASA Marshall Space Flight Center

John Baker, Philippe Adell, Frank Picha, Matthew Kowalkowski
Jet Propulsion Laboratory, California Institute of Technology

E. Glenn Lightsey
Georgia Institute of Technology

ABSTRACT

The Lunar Flashlight Propulsion System (LFPS) was developed as a technology demonstration to enable the Lunar Flashlight spacecraft to reach Lunar orbit and to desaturate onboard reaction wheels. While the system produced over 16 m/s of delta-v and successfully managed momentum, variable thrust performance, most likely due to debris in the propellant flow path, kept the spacecraft from reaching the Moon. This paper details the in-flight journey of the LFPS, highlighting both successes and challenges met throughout the mission, and provides lessons learned applicable to future CubeSat missions and additively manufactured propulsion systems.

INTRODUCTION

Lunar Flashlight (LF) was a NASA Jet Propulsion Laboratory (JPL) technology demonstration mission with a science goal of investigating the distribution of surface ice deposits on the Lunar south pole. It was developed and managed by JPL, with the NASA Marshall Space Flight Center (MSFC) leading development of the propulsion system. The Georgia Institute of Technology (GT) Space Systems Design Laboratory (SSDL) designed and integrated the propulsion system and served as the home of the mission operations team. The science team was comprised of scientists at the University of California, Los Angeles (UCLA), the University of Colorado Boulder (UC Boulder), the Johns Hopkins University Applied Physics Laboratory (APL), and the NASA Goddard Space Flight Center (GSFC). The Georgia Tech Research Institute (GTRI) performed final integration and test activities.

Spacecraft Overview

As a 6U CubeSat, Lunar Flashlight was developed to demonstrate a number of new technologies within a small form factor. It exhibited new propulsion system technologies including ASCENT pro-

pellant (AF-M315E), a green monopropellant developed by the Air Force Research Laboratory (AFRL) as a safer alternative to hydrazine. Lunar Flashlight also acted as a demonstration of metal additive manufacturing applied to propulsion system primary structures.¹ The science payload validated the concept of compressing near-infrared laser reflectance spectroscopy into the CubeSat form factor.²



Figure 1: Integrated Lunar Flashlight Propulsion System Prior to Launch

The novel propulsion system (Figure 1), developed by GT and MSFC, was expected to perform the mission trajectory correction maneuvers (TCMs), Lunar orbit insertion, and momentum management burns. The attitude control system (ACS) for

the spacecraft, a Blue Canyon Technologies (BCT) XACT-50, would command the propulsion system to place the 13.3 kg spacecraft in a near-rectilinear halo orbit around the Moon. This, along with the near-infrared laser and detector, would allow LF to complete its science goal of addressing one of NASA’s Strategic Knowledge Gaps: the composition, quantity, distribution, and form of water/H species and other volatiles associated with Lunar cold traps.³

Although thrust reliability issues prevented Lunar Flashlight from reaching Lunar orbit, the mission successfully demonstrated all onboard technologies. The Lunar Flashlight Propulsion System (LFPS) was able to impart about 16.2 m/s of delta-v, confirming its intended functionality. The near-infrared laser and detector science instrument conducted multiple experiments, successfully demonstrating performance of the design in space. Additionally, all other subsystems operated nominally throughout the mission.

Propulsion System Design

The LFPS uses four 100 mN thrusters located at the base of the spacecraft (Figure 3). All thrusters are mounted in the axial direction but canted inward allowing for delta-v capability and momentum management. It is a pump-fed system, using an electric gear pump to pressurize propellant to the operating pressure required by the thrusters. The propulsion components are mounted to a 3D-printed titanium distribution manifold, which also serves as a major structural component of the propulsion module.^{4,5}

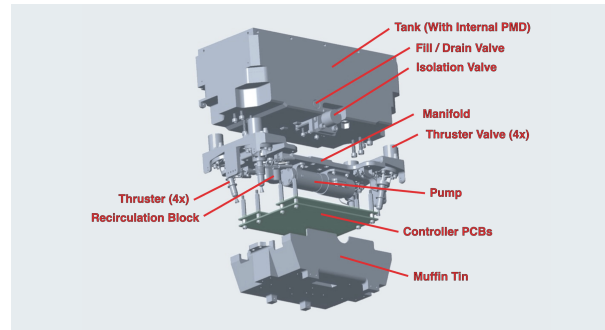


Figure 2: Expanded View of the LFPS

The LFPS is composed of two primary subassemblies, namely the propellant tank and manifold (Figure 2). The propellant tank subassembly includes a two-piece welded structure, as well as various components for propellant management and monitoring. These include a fill/drain valve for propellant loading, an isolation valve for isolating the tank from the manifold, a propellant management device (PMD)

for capturing the propellant in zero-g, a filter to restrict large particles from flowing out of the tank and into the manifold, a tank pressure sensor, and two Kapton heaters for maintaining required propellant temperatures. Additionally, the subassembly includes three thin and flexible thermocouples to monitor tank and heater temperatures.

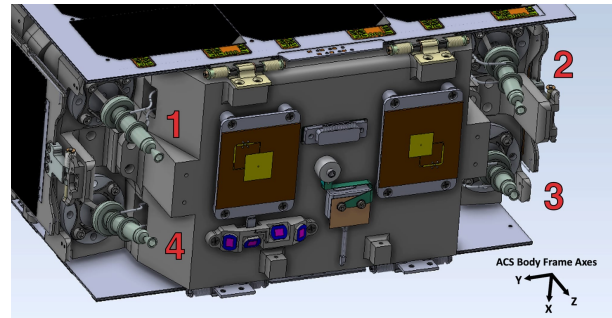


Figure 3: Thruster Positions

The manifold subassembly features a 3D-printed titanium structure with integrated flow passages. Attached to this are four 100 mN thrusters, four thruster valves which control propellant flow to each thruster, an electric propellant pump with a brushless DC motor for pressurizing propellant, a propellant recirculation block allowing pressurized propellant to recirculate while thrusters are not firing, and a pressure sensor. An embedded controller is also attached, which provides propulsion system commanding and telemetry through an RS-422 interface with the XACT.⁶ A 2 mm thick titanium enclosure known as the “muffin tin” is mounted over the controller. This enclosure provides an interface for mounting external components such as low-gain antennas and a sun sensor, and offers thermal protection and radiation shielding to the controller electronics.⁴

Propulsion System Testing

The propulsion system components underwent several tests at various stages of assembly. First, a qualification test program was conducted on non-flight prototype components to assess their physical properties, including burst and leak resistance, and to confirm functional properties such as acceptable pump run time and valve cycle limits. After this, each flight component underwent an acceptance test program before being delivered for assembly, integration, and further testing. The acceptance test was a less rigorous version of the qualification test, aimed at verifying the component’s conformance to specifications and performance requirements. The qualification and acceptance test matrix is shown in Figure 4.

Testing Campaigns	Flight Qualification					Flight Acceptance					
	Radiation Testing	Random Vibration	Thermal Vacuum	Performance Life	Proof & Burst	Random Vibration	Thermal Vacuum	Proof & Leak	Hot Fire	End to End Functional	
Components	100mN Thrusters	--	Qual Levels & Durations	--	Per Test Plan	--	Acceptance Levels & Durations	--	MDP x 1.5	Per Test Plan	FlatSat
	Pump	--	Qual Levels & Durations	Qual Margins (4 Cycles)	Per Test Plan	MDP x 2.5	Acceptance Levels & Durations	Acceptance Margins (4 Cycles)	MDP x 1.5	--	FlatSat
	Solenoid Valve	--	Qual Levels & Durations	Qual Margins (4 Cycles)	Per Test Plan	MDP x 2.5	Acceptance Levels & Durations	Acceptance Margins (4 Cycles)	MDP x 1.5	--	FlatSat
	Fill/Drain Valve	--	Qual Levels & Durations	Qual Margins (4 Cycles)	Per Test Plan	MDP x 2.5	Acceptance Levels & Durations	Acceptance Margins (4 Cycles)	MDP x 1.5	--	--
	Controller	TID & SEE (Prototype)	Qual Levels & Durations	Qual Margins (4 Cycles)	Per Test Plan	--	Acceptance Levels & Durations	Acceptance Margins (2 Cycles)	--	--	--
	Propellant Tank	--	--	--	Per Test Plan	MDP x 2.5	--	--	MDP x 1.5	--	--
	Manifold	--	--	--	--	MDP x 2.5	--	--	MDP x 1.5	--	--
	LFPS System	--	--	--	--	--	SC Protoflight Levels & Durations	SC Protoflight Levels & Durations	MDP x 1.1	--	AITP-09

Legend

- Vendor
- MSFC
- GT
- JPL

Figure 4: LFPS Qualification and Acceptance Test Matrix⁴

After the propulsion system was assembled, it underwent a short test campaign. First, a system flow and leakage rate verification test was completed using helium to show expected flow through the system and lack of system leakage. One thruster (thruster 4) was replaced due to a potentially problematic difference in manufacturing techniques. When this thruster was replaced, the flow test was repeated, but only on the replaced thruster.

Prior to delivering the LFPS subsystem to the LF project, mass, dimensional, and power verification tests were performed, along with an electrical functionality test. All of these tests showed results in acceptable ranges and informed how the system would perform in flight.

Following spacecraft-level integration, the LFPS underwent additional testing.⁷ At various points in the systems integration and test (SI&T) process, a basic functional test was repeated. Each time, this test verified propulsion system communication through the LF Command and Data Handling (C&DH) system and XACT, verified temperature and pressure sensor feedback, exercised heater channels at safe benchtop temperatures, and optionally exercised the valves. Additionally, a post-integration thruster valve commandability test was performed, which verified that the appropriate thruster valve actuated when commanded by the XACT.

The LFPS went through random vibration and thermal vacuum (TVAC) testing as part of the spacecraft-level environmental test campaign. During TVAC testing, thruster preheat cycles were performed during the hot and cold dwells with limited external power. This confirmed that thruster preheat could be achieved at various spacecraft temper-

atures while using a conservative spacecraft power profile. After each environmental test, the LFPS continued to pass its functional test.

A FlatSat was constructed at NASA MSFC to emulate the LFPS system using flight-like spares of the pump, the isolation valve, the controller, a thruster valve, and a thruster. Components analogous to the propellant tank and manifold were included, but they featured different volumes and geometries than the flight design. Hot-fire testing of this FlatSat demonstrated that the included LFPS components could work together as a system to reliably produce thrust.



Figure 5: Propellant Loading Operation

Fueling and final SI&T activities took place at NASA MSFC. During the pre-fueling system functional test, the propulsion system's pump was briefly exercised to ensure the pump and motor driver functioned in their integrated state. During the fueling process (Figure 5), propellant was loaded into the tank through the fill/drain valve, followed by nitrogen pressurant. After performing final propulsion system and other system tests, the spacecraft was loaded into its dispenser for launch.

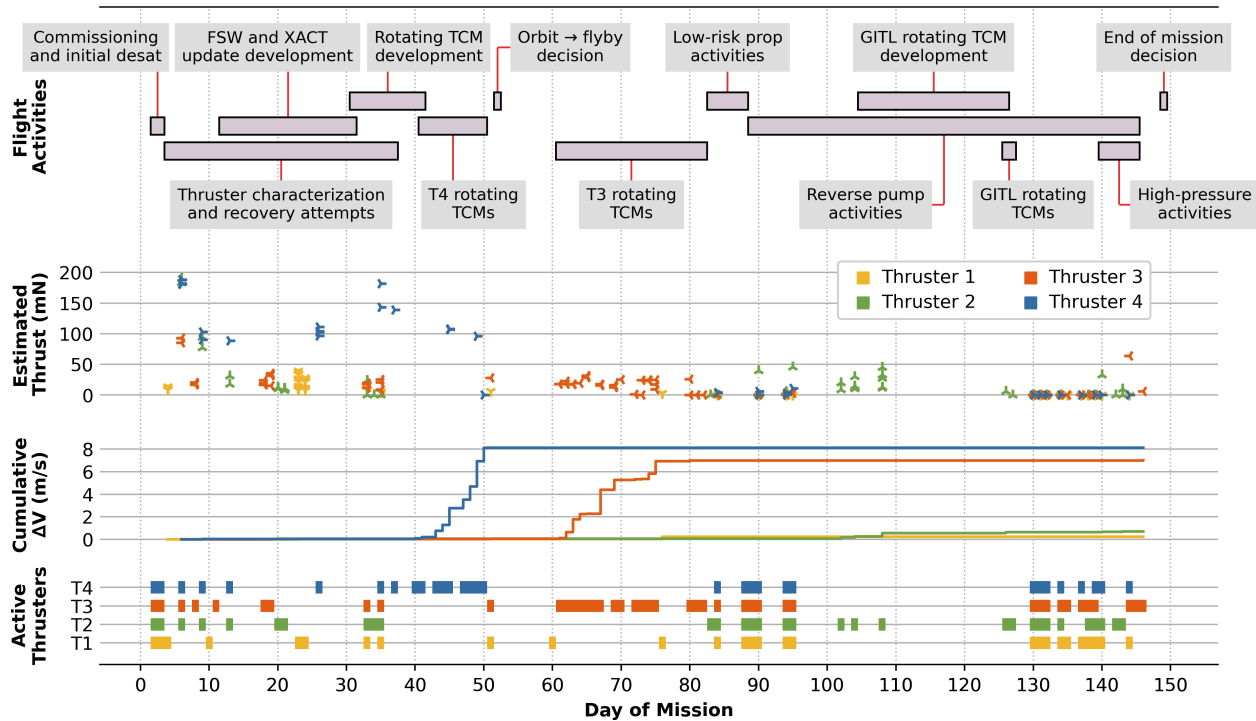


Figure 6: Lunar Flashlight Propulsion System Flight Activities and Performance*

FLIGHT ACTIVITIES

Lunar Flashlight was launched as a SpaceX Falcon 9 rideshare on December 11th, 2022. Following deployment on a translunar trajectory, the spacecraft’s autonomous subsystems activated and placed the system in a stable sun-pointed orientation ready for communication with Earth. Contact was quickly achieved through the Deep Space Network, and telemetry indicated a healthy spacecraft ready for the next stage of the mission.

During the first contact, the propulsion team verified that the propellant tank pressure was within the expected range, indicating that no pressurant or propellant had leaked from the spacecraft in the 10 weeks since propellant loading had occurred. LF was the first green propellant spacecraft to demonstrate loading at a remote servicing facility away from the launch site, and this acted as additional confirmation that this fueling approach can be used successfully by other missions. Other sensor information includ-

ing propellant manifold pressure and system temperatures also indicated a healthy spacecraft propulsion system ready for activation.

The mission plan called for a rapid start to propulsive activities, soon after the initial contact. The propulsion system would undergo fuel priming to evacuate the gas in the manifold and fill it with propellant, followed by thruster commissioning to ease the thrusters into operation. Then, an initial momentum desaturation maneuver would be performed to lower reaction wheel speeds, removing angular momentum imparted by the spacecraft deployment process.

Fuel priming occurred as expected. First, the thruster valves were temporarily opened to vent the manifold to vacuum. Then, the isolation valve was opened, allowing propellant to flow into the manifold. Manifold pressure rose to just under tank pressure, indicating that the manifold was now primed with propellant.

Priming was followed by a thruster commissioning process. This process began with heating all four thrusters, then opening the isolation valve, run-

*This chart displays a timeline of major propulsion mission activities alongside thruster performance and usage. **Estimated Thrust** values were calculated using a combination of system momentum changes and Doppler residual data. Usually, one or more thrust calculations were performed during each event. Thrust often varied based on pulse length and pressure, so this figure provides a general trend of each thruster’s performance over time. **Cumulative ΔV** values were not calculated or assigned to specific thrusters for every maneuver, but virtually all maneuvers with any significant value are captured in this per-thruster summation. **Active Thrusters** are defined by any thruster valve or thruster heater usage on a given day.

ning the pump to raise manifold pressure, and finally pulsing the thrusters 30 times with 50 ms pulses. The first commissioning attempt was aborted due to high system temperatures. A combination of increased temperature limits and a more time-efficient procedure execution allowed the commissioning process to be completed successfully. Although it was not noted at the time, later analysis showed that thruster 1 produced negligible thrust and thruster 3 showed low performance during the commissioning process.

Anomaly Discovery

Following commissioning, the propulsion system was to perform the initial momentum desaturation maneuver, dumping momentum that the onboard reaction wheels were carrying from the initial de-tumble process. The thruster preheat process was performed, and the XACT was commanded to perform the desaturation maneuver. ACS telemetry and Doppler data indicated that thrust had been produced, but perplexingly, the system had entered a higher reaction wheel momentum state. A data review showed that the XACT had commanded thrusters 1, 2, and 3 to fire. The resultant change in angular momentum was consistent with thrusters 2 and 3 producing reasonable thrust, and thruster 1 producing a very small amount of thrust. Additionally, while thruster 2 and 3 were only commanded on for a few seconds at the start of the maneuver, the XACT continued to command thruster 1 to fire until the 60 second maneuver timeout was met (Figure 7). This indicated that thruster 1 was outputting a lower thrust level than expected by the attitude control system desaturation algorithm. An anomaly response team was assembled, which would later grow in size and scope as the team worked throughout the mission to develop methods of obtaining reliable thrust from the system.

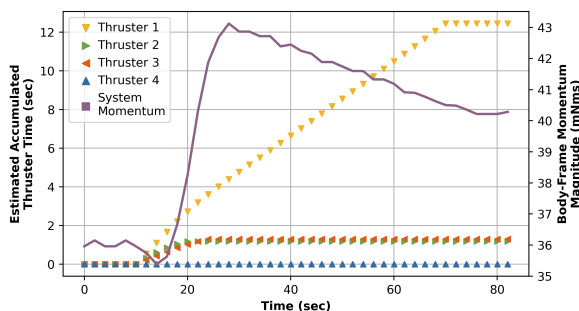


Figure 7: Anomalous Desaturation Maneuver

Initial Characterization and Recovery Attempts

Thruster recovery tests were quickly devised and scheduled with the hope of improving thruster 1’s performance. The actual testing proved to be a slow process due to limited commanding options and concern about saturating the reaction wheels, which would likely result in a loss of spacecraft. Timing (via thruster pulse length), pressure (via pump speed), and temperature (via heater setpoints) were the primary parameters that the propulsion team could modify in an attempt to adjust the performance of each thruster. The initial thruster 1 recovery attempt utilized longer burn times in the hope that additional burn time and propellant flow would “wake up” the thruster. This technique had shown some success in past ground tests, but in this case did not result in any improvement.

Another contact was used to perform 200 ms characterization burns on thrusters 2, 3, and 4 to understand the state of the system. Thrusters 2 and 4 showed essentially equal and nominal thrust performance, while thruster 3 showed about half the nominal performance. Adding to the complexity, momentum and Doppler data from these initial tests showed that thrusters 1 and 3 exhibited a gradual “tail-off” in thrust, rather than sharp impulses.

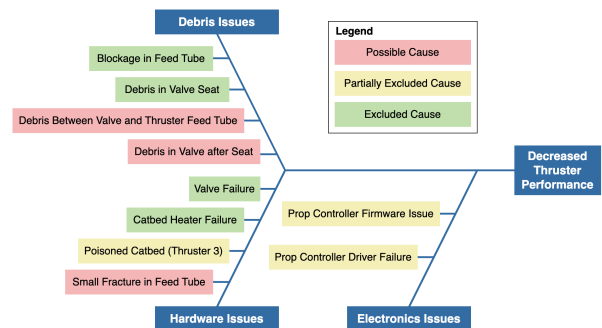


Figure 8: Initial Anomaly Fishbone Diagram

At this point, a fishbone diagram was laid out to track the possible issues on thrusters 1 and 3 (Figure 8). Foreign object debris (FOD) was considered the most likely culprit, but other possibilities were also considered. For example, simultaneous preheating of all four thrusters produced a notable drop in propulsion system voltage, so it was theorized that the voltage delivered to the valves might be too low. A test was performed which disabled thruster heating, then immediately fired the preheated thruster. This ensured sufficient voltage was reaching the valve, but there was no difference in the result.

During these initial recovery and characterization attempts, the Attitude Control System (ACS) and Mission Design and Navigation (MDNav) teams developed tooling to assist in understanding thruster performance. The ACS team utilized telemetered changes in spacecraft body momentum to calculate estimates of thruster performance, while the MDNav team looked at changes in Lunar Flashlight’s two-way Doppler signal. These two techniques allowed the propulsion team to quickly understand the results of thruster firings in real time. In addition to the estimates provided by ACS and MDNav, the propulsion team, or “prop” team, monitored the thermal response of each thruster as well as the manifold pressure response while firing to determine the health of each active thruster. As these monitoring and estimating techniques matured, the propulsion team gained the ability to make real-time decisions while performing flight tests. Figure 9 shows an example of the correlation between Doppler shift, momentum response, manifold pressure, and thruster temperature during a single-thruster momentum desaturation activity.

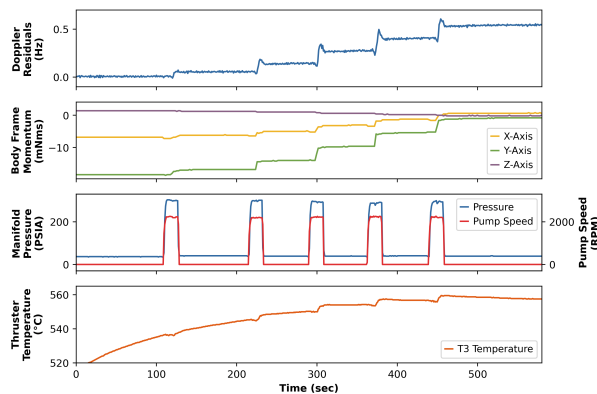


Figure 9: Doppler, Momentum, Temperature, and Pressure Response During a Successful Momentum Wheel Desaturation Activity[†]

With the confirmation that thruster 3 was producing about half the thrust of thrusters 2 and 4, a contact was dedicated to performing thruster 3 “wake-up” activities. This consisted of three 2-second pulses and two 1-second pulses. The momentum change associated with each 2-second pulse

[†]In this activity, five distinct 2-second pulses were executed on thruster 3. Doppler shifts correspond to changes in the line-of-sight component of the spacecraft’s velocity. Larger jumps in the signal indicate greater amounts of thrust. The ACS was commanded to maintain a constant attitude during this activity, but peaks and troughs around each pulse indicate small attitude transients due to the torque of the thruster on the spacecraft. The varying scale of changes in the spacecraft body frame momentum data can also be used to indicate thrust levels. The manifold pressure data indicates some amount of propellant flow. In the middle of each pump run, a small depression can be seen in the pressure, indicating that propellant was flowing through the valve. Finally, each pulse can be identified by a slight increase in thruster temperature. In some cases, propellant flow would cause the thruster to cool, but this data indicates some amount of self-heating due to the catalyzed propellant.

was only about two times greater than what was seen with previous 200 ms pulses, indicating further diminished performance.

An analysis performed by the ACS and MDNav teams showed that with the current trajectory and prop system performance, the spacecraft could still reach Lunar orbit using only thrusters 2 and 4. Further tests were performed to characterize these two thrusters, consisting of 1 and 2-second pulses. Unfortunately, this pulse sequence revealed a quick drop-off in thruster 2 performance, from 94.7 mN to 17.6 mN of thrust.

With thrusters 1, 2, and 3 now performing off-nominally, the recovery efforts widened to include all three thrusters. A new test campaign consisted of repeated short pulses on each thruster while increasing temperature and pressure. Pump speed was gradually increased to target thruster inlet pressures of 175, 260, 320, and 405 psia. These values were chosen because ground testing of the thrusters was often performed at these pressures. Pulses were limited to 1 second at high pressures in case a thruster suddenly “woke up”, which could quickly saturate the momentum wheels. This set of tests generated mixed results. Thrusters generally exhibited a broad drop-off in performance, although increased pressure often led to locally higher thrust. As thruster 2 performance dropped, it did not generate a thrust “tail-off” as seen on thrusters 1 and 3. Two of the 405 psia thruster 1 pulses exhibited significantly less “tail-off”, coupled with an increase in thrust.

These initial thruster recovery and characterization attempts were often cut short due to reaching temperature limits. Each thruster heater could only be left on for about 30 minutes before the corresponding thruster valve temperature would exceed its qualification test limits. In addition, after nearly every thrust-producing pulse, the spacecraft needed to be slewed 180 degrees. This simple alternating pattern allowed momentum build-up from one or more pulses to be cancelled out by other pulses, but each slew could take 90 seconds or more. This meant only a few pulses could be executed per contact, before having to stop and let the propulsion system cool for about 8 hours.

Software and Parameter Updates

While the thruster characterization and recovery attempt process was underway, the propulsion team engaged the flight software (FSW) team at JPL, as well as the XACT manufacturer, BCT, to provide software and parameter updates which would allow for safer commanding of longer and more varied propulsive activities.

The team had determined that the XACT's *ManualBurn* functionality was the best way to manually command burns on each thruster given the anomalous performance. However, this command could not be fully utilized without updates to the XACT. By default, the XACT would perform automatic momentum desaturation burns if system momentum exceeded a threshold while the XACT was configured to run a *ManualBurn* command or any other thruster command. In order to safely run *ManualBurn* commands without risking a problematic automated desaturation burn, this functionality needed to be disabled.

Additionally, the duty cycle used by the *ManualBurn* command was initially set to 90%, meaning the valve would be commanded open for 900 ms each second. The team concluded that varying this duty cycle parameter would open up opportunities for more customized operation of each thruster.

Additional XACT updates were discussed, such as modifying the expected thrust from each thruster, which could allow for the XACT's delta-v and momentum management algorithms to be used if thruster performance remained predictable at reduced levels. A need was also identified to create a momentum safety net, automatically cutting off thruster usage if momentum exceeded configurable thresholds.

This momentum safety net capability was not possible with an in-flight XACT update. Fortunately, it could be implemented on the LF FSW as an in-flight update. Threshold parameters were implemented for each reaction wheel's momentum as well as the estimated system momentum along each axis. If any of these thresholds were exceeded in XACT telemetry, a FSW fault response would disable 12V-nominal power to the propulsion system, closing all valves, stopping the pump, and disabling all heaters, safely placing the system in a deactivated state within seconds.

Prior to the momentum safety net being implemented, the team had to limit burn times so reaction wheels would not be in danger of becoming saturated. The FSW team worked over the December holidays to get this functionality implemented, and

after ground testing was performed by the operations team, or "ops" team, the FSW was successfully patched with the update in early January. This not only gave the spacecraft a momentum safety net, but also demonstrated the mission's first and only in-flight software patch. Around this time, BCT also provided XACT parameter table updates to disable the automatic momentum management functionality and vary the thruster duty cycle.

Longer Recovery Attempts

After the momentum safety net was implemented onboard the spacecraft, longer pulses could be safely commanded. A series of 5, 8, 10, and 30-second pulses were performed on thrusters 1, 2, and 3. Thruster 3 produced enough momentum change to trip the momentum safety net, but none showed improved performance. When thruster 2 underwent this set of longer pulse tests, its performance dropped to 0 mN.

The XACT parameter update allowed the team to execute repeated pulses at specific duty cycles via the *ManualBurn* command. The thruster manufacturer suggested a continuation of 90% duty cycle recovery pulses, as well as 50% duty cycle pulses to match ground testing. This approach was tested on thrusters 1 and 3. Thruster 3 showed some improved performance, but it was inconsistent and too low to be immediately useful. Thruster 4 was also tested at 25% and 15% duty cycle, successfully demonstrating that a higher performing thruster could potentially be matched with a lower performing thruster.

Methods of Performing Trajectory Correction Maneuvers

Although recovery attempts were underway with the new momentum safety net and parameter updates, no appreciable amount of delta-v had yet been generated in-flight – only small momentum management burns had been performed. While these attempts continued, a set of options was developed to document the ways in which trajectory correction maneuvers might be successfully performed, allowing LF to enter orbit around the Moon (Figure 10).

The original mission plans relied on the XACT to perform 4-thruster delta-v maneuvers with little operator intervention. Through a collaboration between MDNav, ACS, and BCT, it was determined that the XACT's *DeltaV* command could still be used in several scenarios, some requiring additional XACT parameter changes. First, if all thrusters recovered to near 100% performance, the project

could utilize the standard *DeltaV* command without adjustment. Second, if all thrusters recovered to above 20%, the XACT’s *DeltaV* mode could be used with modifications to its “expected thrust” parameters. Finally, if any thruster performance dropped below 20% but remained above 6%, additional timing and burn attitude limits would apply due to a likely lack of catalyst bed self-heating. Such a scenario would require constant preheating, placing additional strain on the system battery.

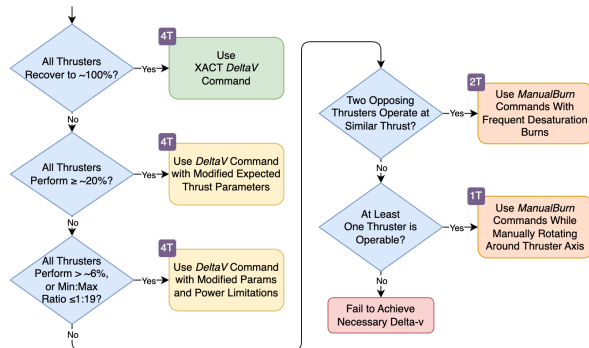


Figure 10: Trajectory Correction Maneuver Options Considered

Below 6%, the system could run into additional limitations, such as the non-adjustable minimum and maximum pulse times of 50 and 950 ms. These values imposed a maximum thruster performance ratio of 19:1, as a higher thrust ratio would require operating at least one thruster longer than 950 ms or less than 50 ms per second. Also, at low enough thrust levels, even with steady performance, the required burn time for a given amount of delta-v would become unreasonable. Assuming autonomous burns were performed around the clock without operators in the loop, the system would still hit thermal limitations of valves and other components, requiring multi-hour cooldown periods between maneuvers.

A more complicated TCM approach was identified, relying on two thrusters and manually timed burns. If two opposing thrusters, either the thruster pair [1, 3] or [2, 4], could be commanded to produce similar thrust, they could be operated simultaneously for short periods of time, limited by z-axis momentum build-up. After building up momentum, the spacecraft would rotate approximately 95° to a desaturation attitude and perform a very short desaturation burn to remove the additional momentum. This sequence could repeat multiple times, until system components reached their temperature limits.

A final option was considered, which was to perform TCMs using a single thruster. As long as one thruster remained operable, maneuvers could take place by manually firing the working thruster while rotating the spacecraft around the thrust axis. A major benefit of this approach was that it removed the entire problem of having to balance the performance of multiple thrusters. Balancing two or four thrusters would likely pose an impractically delicate problem of adjusting pressure, temperature, XACT duty cycle and thrust parameters, and would be highly susceptible to performance changes mid-maneuver. The single-thruster approach was much more resilient against mid-maneuver performance changes. While rapid performance changes during a single-thruster burn would affect momentum build-up, the thruster could continue burning in the appropriate direction, and the momentum could be cleaned up with a short desaturation burn performed separately. This option also required much less power, so off-sun TCMs would be less power constrained, allowing the catalyst bed heater to stay on throughout the maneuver.

At the time, thrust levels exceeded the 19:1 ratio required to use the standard *DeltaV* commanding approach. Also, thruster 4 continued to be the only seemingly healthy thruster. Pairing it with the opposing thruster 2 for the two-thruster approach was not viable as thruster 2’s measured thrust was close to 0 mN. As no reliable thruster recovery had been achieved, and the single-thruster rotating TCM option provided many simplifying benefits, it stood out as the most practical way of generating the delta-v required to enter orbit around the Moon.

Rotating TCMs

Development of the rotating TCM technique began with the assumption that the healthy thruster 4 would be utilized for single-thruster maneuvers, although the approach could be generalized to utilize any performant thruster. An important property of the technique was its ability to limit momentum build-up occurring from the thruster’s position on the spacecraft. The primary issue with firing one thruster was that it would impart a torque on the spacecraft, since no thruster’s force vector was aligned with the spacecraft’s center of mass. By rotating at a constant rate around the force vector of the active thruster, momentum build-up occurring at a given angle θ would be mostly cancelled out when the spacecraft was at the opposite angle $\theta + 180^\circ$, assuming constant thrust (Figure 11).

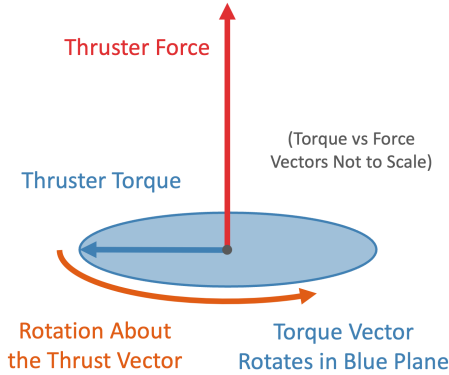


Figure 11: Simplified Drawing of Thruster Torque in the Inertial Frame. As the Spacecraft Rotates, Little Net Torque is Produced⁸

This notional model matured into a usable design as a result of consultations, analysis, and simulations across the MDNav, ACS, and prop teams. For example, a core requirement of this technique was to rotate the spacecraft at a constant rate around a custom axis using reaction wheels. This had not been performed in-flight, so the appropriate XACT attitude command had to first be identified, then validated on the system testbed.

Selecting the rotation rate required balancing reaction wheel momentum and torque limits with propellant management considerations. A rotation rate of $6^\circ/\text{s}$ was ultimately adopted as it offered simplifying advantages. First, this rate performed a full revolution in one minute, providing a convenient time reference for maneuver planning. Second, the chosen rate was a round number that fell comfortably within reaction wheel and propellant management limits.

The propellant tank assembly included a propellant management device (PMD) which utilized surface tension to keep propellant at the tank outlet during zero-gravity operations. If radial acceleration was too high, propellant could be flung away from the PMD, allowing nitrogen pressurant to escape from the tank, which could be a mission-ending event. Analysis of the tank geometry had been performed that indicated the PMD would stay wetted while rotating at $6^\circ/\text{s}$ and firing. The analysis suggested an expected 0.3 mm/s^2 to 0.6 mm/s^2 of radial acceleration, far less than the 3 mm/s^2 that the PMD sponge was designed to withstand.

The reaction wheels were responsible for managing spacecraft rotation and responding to torque from thruster pulses. This created a limitation on the amount of thrust that could be safely generated. At $6^\circ/\text{s}$, the reaction wheels maintained an average thrust-handling capacity of about 26 mN. Consider-

ing that thruster 4 continued to operate at a nominal thrust of about 100 mN, a duty cycle of 25% was selected. This would allow for an acceleration along the thrust vector of approximately 2 mm/s^2 , or about 2.4 m/s of delta-v during a 20-minute burn.

A few complicating factors were also considered. First, to keep momentum wheel limits from exceeding safe thresholds during the burn, a momentum preload was needed. This was accomplished by performing a 60° “setup burn” while rotating, to “kick” the momentum out to the appropriate position in the torque plane. A “main burn” of up to 20 minutes would then execute, followed by a 60° “take-down burn” to bring momentum back close to its starting position.⁸ Also, a feedforward torque value was developed for use by the ACS, allowing the XACT to counteract expected torque from the burning thruster.

Once these primary operational constraints were determined, work began on developing rotating TCM command sequences, with an emphasis on scripting and autonomy so that three of these burns could be performed autonomously each day. Each maneuver would require its own sequence, responsible for configuring the propulsion system, placing the spacecraft in the appropriate burn attitude, and commanding appropriately timed rotations and burns. Rather than manually develop each sequence, time was taken to develop tooling which could quickly produce maneuver command sequences, given inputs such as thruster number, desired delta-v attitude, and burn duration. The development timeline was highly compressed, taking less than one week to evolve from concept to delta-v-producing flight activity.

Before executing each rotating TCM command sequence in-flight, a set of verification and validation (V&V) steps was taken on the ground. First, parameters from the generated sequence were passed into a momentum simulator along with the current momentum state. This simulation would verify that with nominal thrust, onboard momentum safety net thresholds would not be exceeded. Second, the sequence was executed on a testbed to ensure that it would properly and safely command each system during the maneuver.

Thruster 4 Rotating TCMs

On the spacecraft, iterative steps were taken to prove the rotating TCM technique. First, a 55° off-sun pulse test was performed, showing that the spacecraft’s power system could handle thruster pre-heat and firing while not fully sun-pointed. Second,

a spin-up and spin-down test demonstrated that the spacecraft could be rotated at $4^\circ/\text{s}$. This was followed by a test demonstrating a 20-second burn of thruster 4 at 15% duty cycle, while still rotating at $4^\circ/\text{s}$. Next, the main burn time was increased to 60 seconds and the rotation rate was increased to $6^\circ/\text{s}$. Finally, a 5-minute main burn was performed at $6^\circ/\text{s}$. Later maneuvers would reach 20 minutes in main burn length and would utilize a 25% thruster duty cycle.

The x/y momentum plot in Figure 12 represents a close-to-ideal rotating trajectory correction maneuver. In it, the three burn phases (setup, main, and takedown) are clearly visible, with thruster 4 demonstrating fairly stable performance throughout the maneuver. The stable performance resulted in the final x/y momentum returning very close to the initial momentum. While the 15% duty cycle main burn lasted only 5 minutes, it resulted in approximately 0.51 m/s of delta-v. Telemetry from this maneuver can also be seen in Figure 13.

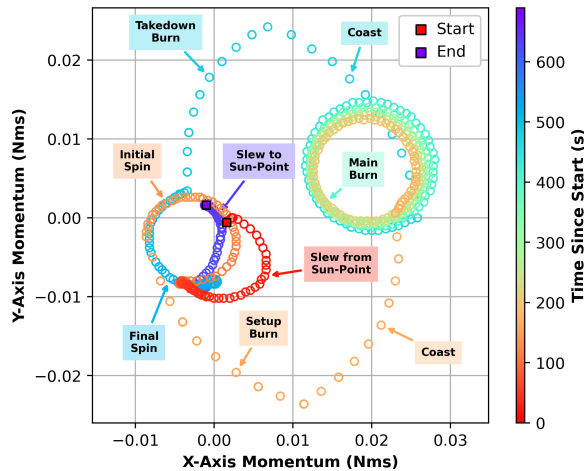


Figure 12: Spacecraft Body Frame X/Y Momentum Plot During Thruster 4 Rotating TCM #3

Subsequent main burns were executed at 10, 15, and 20-minute lengths. Resulting data indicated that longer burns produced less average thrust, as thrust dropped off over the course of each maneuver. The highest-performing maneuver took place

[‡]This is a prime example of a successful rotating TCM activity. Doppler and momentum indicate steady thrust. Thruster 4 rarely showed any signs of self-heating, even when producing nominal thrust, and this activity was no exception. The thermostatic control loop can be seen driving the temperature between 440°C to 450°C . A slight decrease in the thermostatic rise time could be indicative of small amounts of self-heating. During live rotating TCM activities, Doppler measurements showed a considerable sinusoidal component. This was due to antenna motion caused by the 1 RPM rotation of the spacecraft. The data used in this plot was post-processed to remove these antenna motion artifacts from the rotating TCM portion of the activity.

[§]“Thruster Seconds” are dependent on thruster duty cycle. For example, it would take 4 seconds of burning at 25% duty cycle to accumulate one thruster second.

in the eighth thruster 4 rotating TCM, where a 20-minute 25% duty cycle main burn produced 2.2 m/s of delta-v.

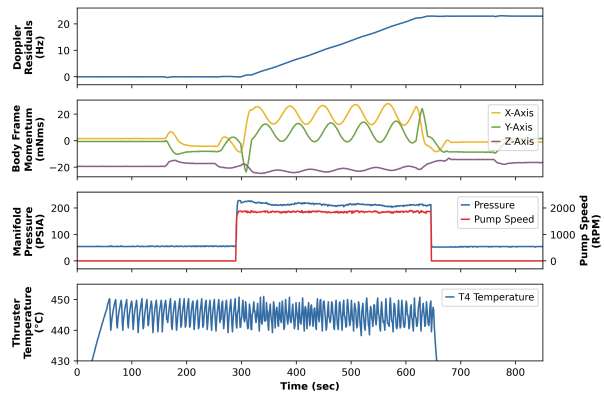


Figure 13: Thruster 4 Rotating TCM #3 (0.506 m/s of Delta-v)[‡]

Occasionally, as momentum built up, a single-thruster desaturation burn, or desat, was executed. If, at the end of a rotating TCM, the momentum levels seemed too close to the safety net thresholds to reliably perform another maneuver, the operations team would use the current momentum data to compute a single-thruster desaturation attitude. A command sequence was then generated to preheat, slew, and fire an appropriate number of thruster 4 pulses to bring the reaction wheel momentum close to zero.

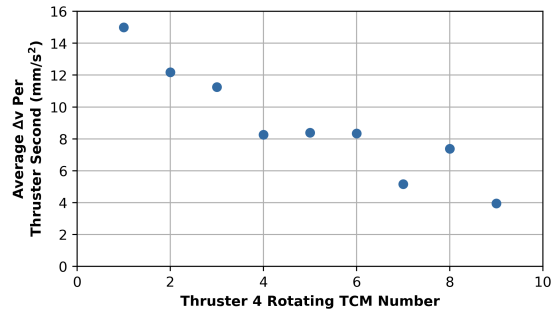


Figure 14: Thruster 4 Rotating TCMs: Average Delta-v Produced Per Thruster Second[§]

This pattern of rotating TCMs and desats continued for over a week. Figure 14 shows a downward trend of thruster performance over this period. Eight maneuvers were executed nominally, but

about halfway through the ninth maneuver, thrust quickly dropped to near-zero levels. In the next contact, the team tried to perform a desaturation burn, but this also resulted in very little thrust.

In total, thruster 4 had produced approximately 8 m/s of delta-v in 91 minutes of main burn time, using the basic rotating TCM design. However, this latest loss of performance meant it was no longer feasible to keep producing the daily delta-v necessary to keep the spacecraft on its Lunar orbit trajectory. Armed with the latest thruster performance data, the MDNav team developed a new low-thrust trajectory design with the hope that LF could be brought into a high Earth orbit. There, it might perform a series of Lunar flybys in 2024.

Thruster 3 Rotating TCMs

The latest thruster data showed that thruster 3 was now the highest-performing thruster, capable of producing 30 mN, so it was selected for use.

The new trajectory called for thrusting in a fully off-sun direction, meaning that the solar arrays would not be generating any power. A series of tests was performed to make sure spacecraft power would stay in a safe range, thruster preheat would maintain an operable temperature, and communication would continue reliably while operating at this new attitude.

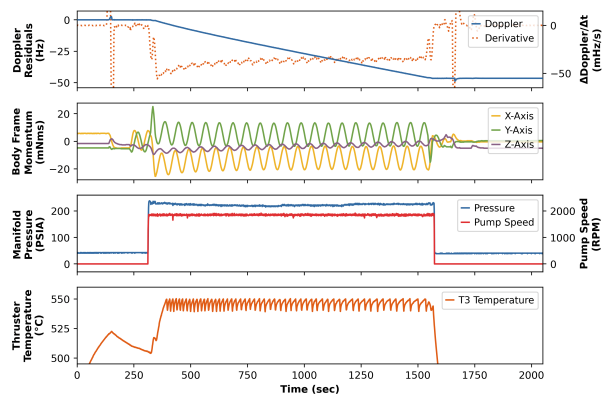


Figure 15: Thruster 3 Rotating TCM #8 (1.17 m/s of Delta-v)[¶]

The operations team was able to easily start developing thruster 3 maneuver sequences, since the existing tooling had been built to support the thrust vector of any of the four thrusters. A few small

[¶]Thrust remains steady throughout most of this rotating TCM, although there is some drift in momentum amplitude at the start of the maneuver, indicating a change in thrust. This is corroborated by the filtered derivative of the Doppler data. Self-heating of the thruster is apparent. A short drop-off in temperature at the beginning of the maneuver is due to the 60° delay between setup and main burns. Small disturbances in the Doppler measurements at the beginning and end of the activity are due to antenna motion, when the spacecraft slewed to the burn attitude, then back to sun-point. Although rotating TCM antenna motion was mostly processed out of this Doppler data, remnants are visible in the derivative.

changes were made. For example, the prop team decided to operate thruster 3 with higher preheat settings, hoping for better performance. Additionally, because this thruster was producing less thrust, the duty cycle was raised from 25% to 50%, and eventually 70%, to better utilize the torque-handling capability of the reaction wheels.

Performance of the thruster 3 TCMs was highly varied. For example, during one 20-minute burn, thrust varied from 25 mN down to only 9.5 mN. This behavior may have been caused by FOD movement due to the motion of the propellant, pump, and thruster valve during the maneuver. Figure 15 shows an example of one of the steadier TCMs performed with thruster 3.

Self-heating behavior also differed widely. Initial maneuvers exhibited a steady moderate amount of thruster self-heating. Thruster temperature would drop as the spacecraft went off-sun, and this self-heating allowed the thruster to return to its thermostatic preheat setpoints once the burn began. However, over the course of several burns, this self-heating behavior became less and less effective, eventually being unable to maintain the preheat temperature (Figure 16). This signaled a lack of propellant reaching the thruster. The self-heating behavior then returned erratically, sometimes performing very closely to what was expected from ground testing, exceeding 800 °C.

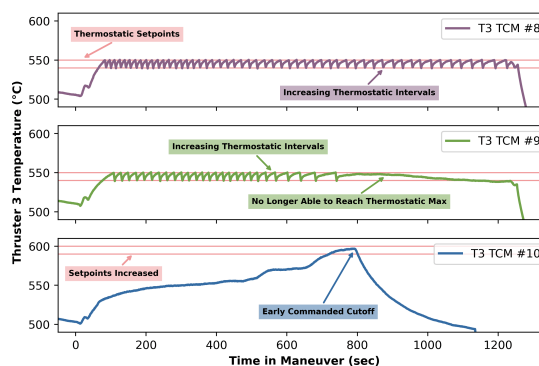


Figure 16: Erratic Thruster 3 Thermal Responses

Initially, 11 TCM burns were executed successfully using thruster 3. This generated about 5.2 m/s of delta-v over 99.5 minutes of burn time. During these maneuvers, a general decrease in thrust was seen, corresponding to less delta-v per maneuver

(Figure 17). Raising the maneuver length to 20 minutes and duty cycle from 50% to 70% increased the delta-v produced in a given maneuver time, but the downward trend continued. Variability during maneuvers caused momentum build-up, even triggering the automated momentum safety net threshold response once. This behavior necessitated multiple momentum desaturation activities.

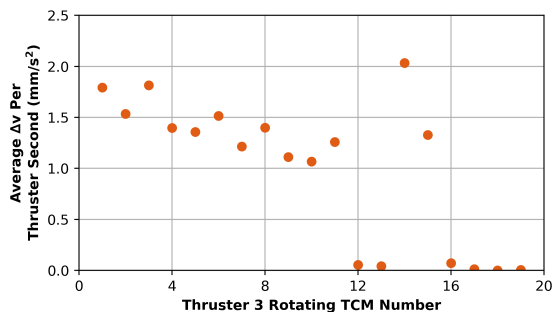


Figure 17: Thruster 3 Rotating TCMs: Average Delta-v Produced Per Thruster Second

The single-thruster rotating TCM approach placed heavy usage on the active thruster valve. At the current rate of valve cycling, the thruster 3 valve would exceed its qualified cycle limit well before the necessary delta-v was generated. Previous ground testing indicated that the valve would eventually fail to open, due to galling from repeated cycling. This prompted the team to change from 1Hz ACS-commanded pulsing to a FSW-commanded approach that would leave the valve open for the entire burn at 100% duty cycle. Thrust could still be adjusted to stay within reaction wheel limits by modifying the pump speed, but since thrust levels had fallen below 20%, the pump was left to operate at the commonly used 1,900 RPM speed.

The initial use of this 100% duty cycle approach started off somewhat nominally for almost a minute. But then, performance quickly dropped to almost zero thrust, where it remained for the rest of the maneuver. It seemed likely that FOD had almost completely occluded the propellant pathway, possibly enabled by the different dynamics of steady rather than pulsed propellant flow.

A decision was made to return to the 70% pulsed operation mode, with the hope that valve cycle limits could be eventually managed some other way. The next maneuver produced a very small but steady trend in Doppler data, but during the entire 10-second takedown burn, a very large trend was identified, corresponding to about 24 mN of thrust. This marked a very clear recovery in thruster performance, although it was unclear if it would last, or if it could be repeated.

The next two maneuvers generated an additional 1.5 m/s of delta-v, but performance was inconsistent, and dropped to near-zero in subsequent tests. Various techniques were implemented in an unsuccessful attempt to deal with this behavior, such as alternating one minute of thruster pulses with one minute of rest, over a 20-minute burn. Eventually, no thrust could be measured at all. The team also attempted burns with thrusters 1 and 2 during this period, with no results usable for delta-v. This meant that no thrusters were currently usable for anything other than low-performance momentum management burns. Such burns weren't strictly necessary, as the operations team had successfully demonstrated momentum desaturation utilizing solar radiation pressure.

Pump Reversal Activities

The concept of reversing the pump had been discussed in the past as a last-resort method of trying to recover thruster performance. Other lower-risk options had always been selected, but now, with no way of producing useful delta-v, the team took a closer look at this higher-risk approach.

The pump was designed to flow liquid in one direction, and only tested in that forward direction. If the pump could run in the opposite direction, it was theorized that this might perturb built-up FOD enough to allow more propellant to flow to thrusters.

In early March, while thruster 3 rotating TCMs were still ongoing, the team requested feedback from the pump manufacturer on the feasibility of safely spinning the pump backwards. They provided suggestions on what speed to run the pump, the expected behavior if FOD entered the pump, and other results the team might expect to see from this mode of operation.

As this capability had never been tested on the pump, a test stand was set up at MSFC with a flight-like pump, pressure system, and controller. A common stand-in for ASCENT, ethylene glycol, was used for this benchtop test. One considered approach was to run the pump forwards, then command it immediately backwards, then forwards again, for a maximum amount of change in pressure. The pump was magnetically coupled, so an initial concern was that this directional "slamming" would cause it to temporarily decouple, if the motor controller could even manage such a rapid change in speed. Fortunately, test stand results indicated that the pump and controller could reliably handle a quick change from +2000 RPM to -2000 RPM without decoupling.

A risk assessment was also performed. One risk was damage to the pump gears if FOD was ingested from the recirculation block, which would result in a loss of propellant pressurization capability. Another risk was valve damage. If the FOD was located between a thruster valve and thruster, reverse pressure could allow FOD to move back into the valve where it might restrict the valve from fully closing, introducing a leak. A leak could be contained by closing the isolation valve, so this would not put the entire spacecraft at risk.

While performing benchtop tests and compiling the risk assessment for the reverse pump activity, a few low-risk activities were performed on the spacecraft to continue testing all four thrusters. This included heating the propellant tank in an attempt to reduce the viscosity of the propellant, as well as performing 10-second sets of pulses at multiple manifold pressures. The highest performance was seen from thruster 4, but it was still not enough to produce useful delta-v.

The first in-flight pump reversal activity characterized pump performance at -1000, -1250, -1500, and -2000 RPM, interspersed with forward runs to verify operability. Additionally, each thruster was individually pulsed while running the pump at -1000 RPM. The next activity again pulsed each thruster, this time running the pump at -2000 RPM, then performed a normal forward pulse train to check for any change in performance. No improved thrust was seen from any thruster.

These pump reversals proved that manifold pressure could be brought below the pressure sensor’s operating range, but no pump activity could be expected to create negative pressure against the vacuum of space. Still, there was a desire to produce a negative pressure differential across the FOD which might pull it away from the downstream orifice it was blocking. It was speculated that if enough propellant made it through the blockage, into the pre-heated thruster, the resulting thrust chamber pressure could be high enough to induce a negative pressure differential across the FOD. This would likely require quickly changing from a forward-pump “thruster-feeding” mode into a reverse-pump “manifold-pressure-reducing” mode.

¶This chart shows six pump reversals, indicated by the lowest manifold pressure measurements. In multiple cases, the pre-timed pump reversals can be seen interrupting periods of good thrust. The manifold pressure sensor is not accurate at low pressures; the lowest pressure readings in this data correspond to zero counts on the analog-to-digital converter (ADC). The pump speed telemetry is unsigned, but out-of-family speed measurements are briefly seen at a few points where the pump switched from +2000 to -2000 RPM. The first two pulse trains show brief dips in thruster temperature, indicative of propellant entering the thruster catalyst bed, and temporarily cooling it. Since little delta-v was achieved in this activity, the antenna-motion-induced Doppler shifts during slews are much more pronounced at both ends of this graphic. Similarly, some artifacts of the 6 °/s rotation survived the Doppler post-processing step.

While this pump “slamming” sequence was being prepared, a simpler test that pulsed the thrusters while running the pump in reverse succeeded in generating thrust from thruster 2. This marked the first time that a specific recovery activity had clearly yielded significant recovery in thruster performance. The first forward-pump pulses resulted in about 30 mN to 50 mN of thrust, but subsequent pulses demonstrated negligible thrust.

A desaturation burn was completed successfully, using a combination of reverse and forward pump rotation similar to the previous recovery test. During the next prop activity, the pump “slamming” operation was executed. This performed 20 forward-pump pulses on all thrusters at 2000 RPM, followed by 20 reverse-pump pulses at -2000 RPM. Here, a pause was built in to allow the PMD to rewet if it had become uncovered by the reverse pressure of the pump. Then, 20 additional 2000 RPM forward-pump pulses were executed. The initial forward pulses showed good performance of 45.5 mN, and after “slamming” the pump, thrust was briefly seen. Unfortunately, the burn was cut short by the onboard momentum safety-net fault response.

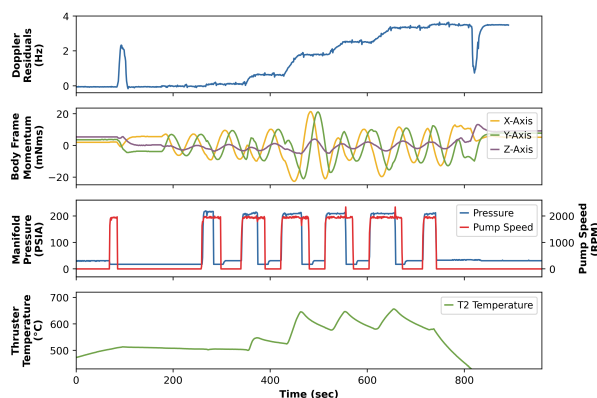


Figure 18: Rotating TCM with Pre-Timed Pump Reversals (0.09 m/s of Delta-v)[¶]

Overall, the improved performance indicated that with a system of properly-timed pump reversals, longer rotating TCMs might be possible once again. This was first tested with a rotating TCM command sequence using pre-timed reversals (Figure 18). After 20 seconds of forward-pump pulsing, the pump would “slam” to -2000 RPM for 15 sec-

onds. This cycle repeated throughout the maneuver with 20, 30, and 40-second burns. The 9-minute maneuver produced over 0.09 m/s of delta-v, but it was clear that the pre-timed reversals were negatively impacting performance, which varied from 20.2 mN down to 8.8 mN. Reversals would interrupt a period of good thrust, and once the next forward-pulsing period began, lower thrust was often seen. Two additional rotating maneuvers were performed with variations in timing, together producing about 0.19 m/s of delta-v, but it was apparent that the rigid timing of pre-compiled command sequences, with no branching logic, was not sufficient.

To work around this problem, the operations team quickly implemented a ground-based commanding system which allowed operators to manually command pump reversals and burns during a rotating TCM (Figure 19).⁹ Maneuvers were still backed by an onboard command sequence, which configured the ACS and prop systems and performed standard tasks such as thruster preheating and spacecraft rotation. Once the spacecraft was spinning, operators could manually command burns and pump reversals while following a decision flowchart. At startup, the ground-in-the-loop (GITL) tool would perform a latency calibration, allowing it to accurately schedule the uplinking of commands, such that they executed at the appropriate onboard rotation phase.

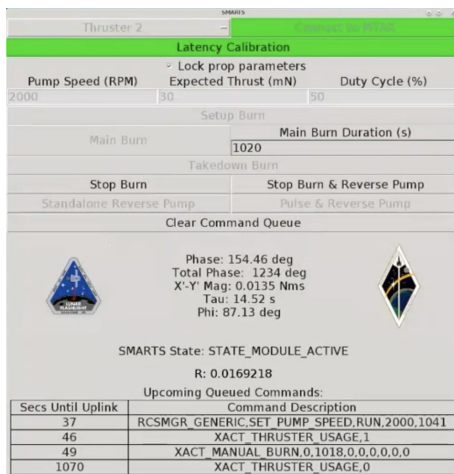


Figure 19: First Use of the Ground-In-The-Loop Tool to Perform a Rotating TCM

After the tool was developed and tested iteratively through a combination of testbed and in-flight activities, it was utilized to perform a GITL rotating TCM. Performance was initially strong, but thrust dropped towards zero over several minutes. Following the decision flowchart, operators performed a reverse pump operation, then restarted the main burn.

Performance remained negligible. Another pump reversal cycle was performed, and little to no thrust resulted. This continued through the rest of the 20-minute rotating burn time allotted by the background command sequence. In all, only 0.089 m/s of delta-v was produced, and the thrust level dropped to under 5 mN on the active thruster 2. Another GITL rotating TCM was attempted, with no resulting thrust.

Over the next two weeks, additional pump reversal activities were performed, as well as high-temperature tests, with negligible resulting thrust. Thruster valves were also commanded open for minutes at a time, without preheating, which showed no signs of propellant flow. The pump reversing method had proven to be less reliable than originally hoped.

Maximum Pressure Testing

With mixed results from the pump reversal technique, the propulsion team introduced maximum pressure testing, another higher-risk method of getting propellant to the thrusters. Throughout the mission, the spacecraft had already demonstrated that higher pump pressure often led to higher thrust. In some notable cases, likely when the flow path for a particular thruster was completely clogged, high pressure did not make a difference. However, the LFPS had not yet been operated in flight to its maximum pressure limits, as this represented a fairly high risk to the system, especially the pump.

System design and test records were reviewed to determine the maximum safe pressure. As the lowest burst pressure test result of any pressurized component was approximately 1250 psia, this was selected as the upper limit for the upcoming activities. A combined forward and reverse pump firing sequence would be executed with varying forward pump speeds, starting at 5000 RPM and continuing higher until a power, decoupling, or pressure limit was reached. The pressure limit was only an analytical limit based on the prop team's analysis of pump RPM vs pressure, as the manifold pressure sensor could not report accurate values at these elevated pressures.

The activity risk assessment noted a few concerns. Components, including the valves or pump, could change performance or stop functioning, which might render the propulsion system unusable. High power draw from the pump could cause the spacecraft to enter safe mode, although this would be straightforward to recover from. High pressure might clear a blockage, causing high thrust which could overwhelm the reaction wheels and cause a

permanent loss of the spacecraft. Finally, a leak or rupture could develop. This would likely not result in a loss of spacecraft. The thruster inlet tube was identified as the most likely component on the thruster to burst, but no test data was available. This would be of low consequence to the rest of the spacecraft, as propellant flow would still be controlled by two upstream valves.

The first test attempted high pressures on thrusters 4, 2, then 1, where forward pump speeds of up to 7000 RPM were tested. The team learned that stepping speeds up slowly was the most reliable way to reach these speeds, as the motor driver would often register an overcurrent fault if a large speed delta was commanded. Thruster 2 demonstrated improved thrust, providing 33 mN of thrust during one pulse train.

Following a successful thruster 2 desat activity, performed at standard pressure with pump reversals, a human-in-the-loop rotating TCM was performed using the same thruster. This TCM utilized higher pump speeds of 3000 up to 7000 RPM, bringing the manifold pressure above the range of the 750 psia pressure sensor. Unfortunately, this only produced 0.01 m/s of delta-v.

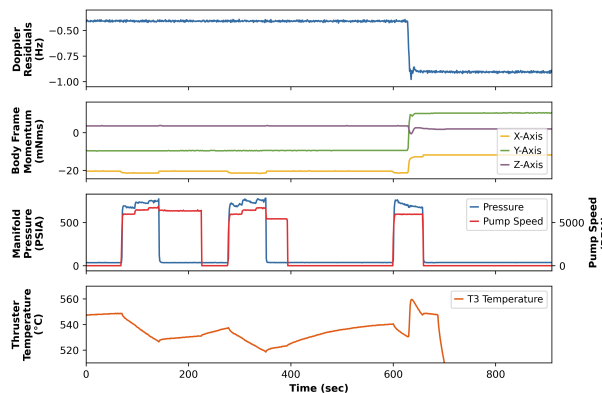


Figure 20: Thruster 3 High-Pressure Test (0.01 m/s of Delta-v)**

Another similar set of tests was run on thrusters 1, 3, and 4. Only thruster 3 had any response (Figure 20), so the test was repeated on thruster 3. First, a pulse train was attempted at 3000 RPM, resulting in no thrust. Following a pump reversal, the pump speed was raised to 5000 RPM, and a burn was attempted. This resulted in a rapid temperature drop,

**This data shows three high-pressure attempts at producing thrust. The last attempt shows a noticeable response in Doppler, momentum, and temperature. The first two attempts used a stair-step pattern to bring the pump speed from 6000 to 7000 RPM. Both times, the command from 6750 to 7000 RPM caused the magnetically coupled motor to become temporarily decoupled. For the third attempt, the pump was left at the initial 6000 RPM speed. Thruster temperature drops are visible whenever the pump was turned on. This was due to voltage drops from the high current draw of the pump, which caused less power to be available to the thruster heater. Small changes in the x-axis momentum plot correspond to pump activity. This is due to angular momentum stored in the spinning pump.

along with a drop in manifold pressure. The momentum and Doppler responses indicated a propulsive event, but it was not in the direction expected of a firing thruster, indicating that propellant had taken an abnormal path out of the system. It was surmised that thruster 3's feed tube had likely fractured as a result of the extremely high pressure and FOD.

One more activity was undertaken to characterize the new behavior of thruster 3. During this activity, a small amount of thrust was detected during the preheat process, indicating that some propellant had collected downstream of the valve, potentially on external faces of the system. Each time the valve was opened, a small amount of momentum response was seen as well as a dip in manifold pressure, but it was not in a predictable or useful direction. After the preheat propellant burn-off process, when the thruster valve was closed, no thrust was measured. This indicated that no leak had developed in the valve. This also strongly pointed towards FOD as the source of the anomaly. It seemed that the extreme pressure and thruster feed tube fracturing had moved the FOD such that more propellant could now flow.

No thrusters were performing well enough to produce useful delta-v, and penalty delta-v was starting to accrue if the Lunar flyby trajectory was to be maintained. At this point, early in May, the project officially decided to call an end to the mission, allowing the spacecraft to continue demonstrating the various onboard technologies, but without an opportunity to perform science at the Moon.

After the end of mission, additional functionality was tested onboard Lunar Flashlight. A pump spin-up test confirmed that the pump could still be operated at 2000 and 2500 RPM, and an electronics heater test confirmed that the never-utilized heaters built into the LFPS controller worked as expected.

PROPULSION SYSTEM PERFORMANCE SUMMARY

Over the course of the mission, the LFPS demonstrated the intended capabilities of producing delta-v and managing momentum. However, thruster behavior was highly variable, with a general decrease in thruster performance over time. After identifying this behavior, a team made up of prop, ops,

ACS, and MDNav representatives embarked on a series of attempts to produce useful amounts of delta-v. Starting with thruster 4, the team developed a novel rotating TCM design which produced more than 8 m/s of delta-v. After thruster 4 performance dropped, the team successfully utilized this approach with thruster 3, producing around 6.8 m/s of delta-v. Once this approach lost its effectiveness on thruster 3, the team developed new methods of producing thrust, including reversing the propellant pump. This seemed to produce pockets of negative pressure, occasionally moving FOD and temporarily relieving propellant restrictions. Over 0.6 m/s of delta-v were produced this way. Finally, the system was pressurized to extreme levels using high pump speeds. This yielded approximately 0.04 m/s of delta-v. Figure 6 presents an overview of the system’s performance throughout flight.

The level of effort required to operate this highly variable system had not been anticipated prior to launch. A review of mission data revealed that before the plans for a Lunar flyby were discontinued, 93 out of 166 staffed contacts included a propulsion system activity (Figure 21). This rate of prop-related activities was approximately five times higher than projected by the prelaunch concept of operations.

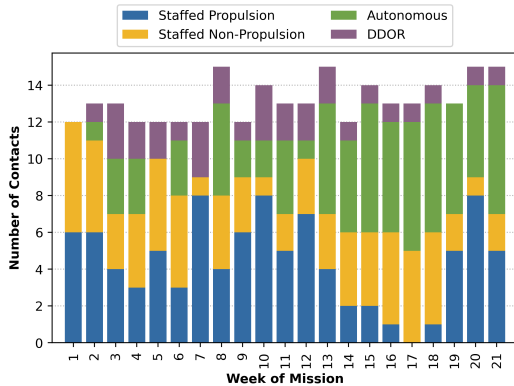


Figure 21: Contact Distribution by Week of Mission

While propellant restrictions overshadowed much of the mission, most system components performed exceptionally well. When not starved of propellant, nominal 100mN performance was seen from the thrusters. The micropump exceeded expectations, running up to 7000 RPM and pressurizing the manifold to above the range of the 750 psia manifold pressure sensor during high-pressure activities. It also successfully operated in reverse, leading to temporary relief of the downstream restrictions. The propellant management device captured propellant and ensured that even during unanticipated rotating burns, propellant remained at the tank outlet.

All valves seem to have performed nominally, even when subjected to higher temperatures and pressures than expected. Finally, the propulsion system avionics controller surpassed expectations. The propulsion anomaly led to operating the electronics for far longer and at much higher temperatures than expected, yet there was no indication of damage, nor any sign of single-event effects. Prelaunch radiation testing⁶ had indicated that total ionizing dose (TID) effects could be measured by comparing a voltage reference to a voltage regulator onboard. This comparison showed no change over the mission, indicating a healthy margin in the TID rating of the LFPS controller.

ANOMALY ROOT CAUSE ANALYSIS

A final fishbone diagram (Figure 22) was developed to identify and investigate potential causes of the low-thrust anomaly and variable thruster performance observed throughout the mission. The final high pressure activity was excluded to avoid influence from the likely thruster feed tube fracture.

Excluded Causes

A blockage within the feed tube was generally excluded throughout the mission because the small diameter of each tube combined with the viscosity of the propellant would have likely caused a complete blockage. Usually, small amounts of thrust were still seen from each affected thruster. The theory of debris in the valve seat was also excluded. FOD in this location would have likely kept the valve from closing completely, which would cause a detectable leak.

Hardware damage due to launch vibration was excluded after MSFC and JPL dynamics engineers reviewed launch load data. This included accelerometer data from the “surfboard” payload adapter, recorded during launch and supplied by the launch provider. A fracture in the feed tube was also considered, but excluded, as thrust would likely be higher than what was seen, and would be in a different direction than the thruster was pointing. Until the last high-pressure activity, all thrust was observed in the expected direction.

Valve mechanical failures were considered, but there was never any indication of a leak, and when valves were commanded open, some thrust and pressure drop was generally detected. It was deemed unlikely that this valve design would open only partially. Similarly, valve electrical failures were discussed, but valve current telemetry was consistent

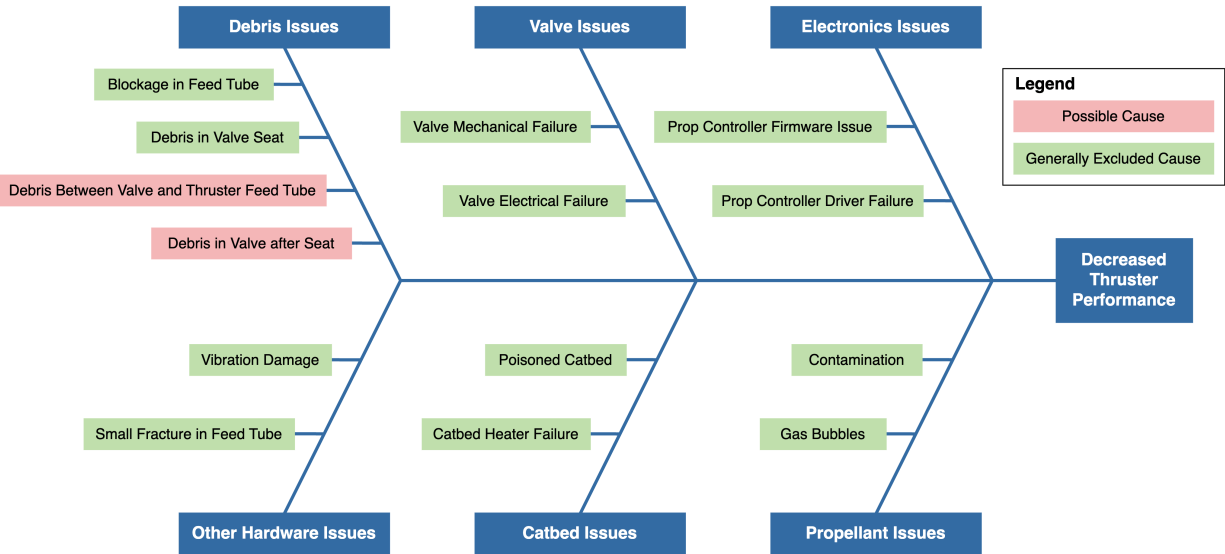


Figure 22: Final Low-Thrust Propulsion Anomaly Root Cause Analysis

with energized valves, and other than tail-off behavior of certain thrusters, thrust levels generally reacted appropriately to valve open and close commands.

Early on, a poisoned catalyst bed, or “catbed”, was suspected. However, in ground testing, poisoned catbeds were observed to reduce thrust by only about 40%, with thrust increasing over time. In-flight performance trended downwards, far below the expected performance of a poisoned catbed. A catbed heater failure was also discussed, but temperature telemetry, preheat timing, and detected thermal soakback indicated nominally operating heaters. Additionally, the spacecraft-level power draw corresponded appropriately with thruster preheats.

Controller electronics issues were also assessed. For example, a propulsion controller driver failure or firmware issue could have kept components from energizing or deenergizing when commanded. These concerns were excluded. Valve commands generally corresponded to dips in manifold pressure and appropriate starting or stopping of thrust. Heater commands corresponded to appropriate temperature telemetry. Power and other telemetry from all on-board systems were consistent with a nominally performing propulsion avionics system.

The idea of fuel contamination was evaluated. While results of a propellant assay are still pending as of this writing, this cause has generally been excluded. Contaminated propellant could lead to lower thruster performance, but would likely not explain the high variability of performance between thrusters. This theory also did not fit well with the

recovery seen during pump reversal activities. Additionally, if debris particles were introduced with the propellant, they would have likely been captured by the tank outlet filter. Gas pressurant bubbles were another possible origin of reduced performance, which could have been induced by PMD performance issues. This cause was also eventually excluded, because longer burns would have flushed out bubbles generated early in the mission, and continued loss of nitrogen would have been indicated by a larger drop in tank pressure over the mission timeline.

Possible Causes

This study highlighted two debris-related possibilities as possible causes of the low-thrust performance that beset the mission. Debris likely became lodged between each thruster valve and thruster feed tube or in the valve after the seat. Both of these scenarios could result in a variable level of decreased flow, and debris in the valve after the seat had been encountered in past ground testing. Figure 23 visualizes the likely locations of this debris. In-flight testing could not definitively prove the location of FOD, but there were certain indications. For example, thrust tail-off was consistent with FOD partially blocking the entrance to the feed tube. In such a scenario, when the thruster valve closed, downstream propellant might temporarily remain pressurized, with pressure and flow rate slowly dropping as propellant dribbled past the blockage into the feed tube over the course of minutes.

The source of the likely FOD was subject to some debate throughout the mission. Early on, one theory was that Krytox lubricant may have been introduced into the propellant flow path during integration of the valves and thrusters, as this had been experienced during ground testing. However, ground testing showed that this would likely have been flushed out or burned off over time. Another theory was that the additively manufactured manifold may not have been cleaned effectively. This was supported by cleanliness issues found with a spare manifold. Finally, it was theorized that particles originating from the printed manifold may have been dislodged by testing and launch vibration loads, as well as operational forces. Investigation of the manifold manufacturing and cleanliness processes led to a number of strong recommendations for future designs.

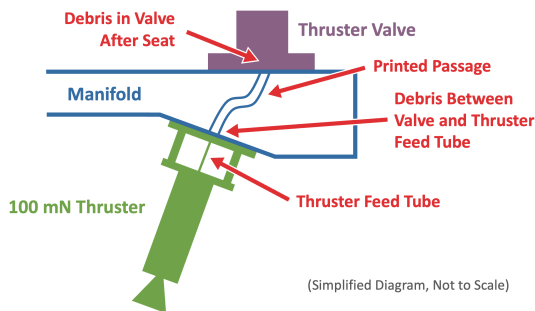


Figure 23: Likely Locations of Debris

LESSONS LEARNED

The successes and challenges faced by this mission provided many lessons applicable to future propulsion system and mission designs. As Lunar Flashlight was originally slated for launch on the first flight of the Space Launch System (SLS), there was schedule pressure to deliver the spacecraft prior to the SLS integration deadline. Changes to the LFPS contract late in the development process resulted in a shortened timeline for designing, testing, and assembling the LFPS. This timeline constraint, along with the project’s technology demonstration classification, led the project to accept more risk during the development process. However, additional risk-reducing activities may have led to a better mission outcome.

Prevention and Mitigation of FOD Contamination

As a technology demonstration, Lunar Flashlight was designed to push the envelope of what is possible with the latest technologies. One of these technolo-

gies was powder bed fusion, used to additively manufacture the LFPS manifold. The most likely cause of the anomalous mission performance was determined to be metal FOD restricting flow out of printed passages in the manifold, which could likely have been avoided through additional prevention and mitigation steps.

Preflight documentation and in-flight performance data was reviewed by NASA MSFC, including additive manufacturing experts, resulting in a number of recommendations. Critically, it was noted that launch and prelaunch vibration loads, along with cyclical pressurization and flow during operations, could dislodge sintered particles, leading to blocked orifices. Buildup around these orifices could be most effectively mitigated through the addition of immediately upstream filters. Shedding could also be controlled by applying a chemical etching surface finish to the printed passages, clearing leftover sintered particles as part of the manufacturing process.

While a propellant tank outlet filter was included in the LFPS, along with a coarse filter in the recirculation block, the lack of additional filters meant that FOD located inside the manifold could still flow towards thrusters, eventually building up propellant-starving blockages. The LF printed manifold underwent a standard cleaning process, but no internal surface finishing process was performed.

Additional inspection and testing steps were also recommended. For example, CT scanning of the manufactured parts could help verify the internal geometry of printed passages and identify trapped powder or FOD left over from machining. While later printed components underwent CT scanning, the LF flight manifold had not been inspected this way. As part of future cleanliness verification processes, it could be useful to vibration test additively manufactured parts at the component level to ensure that they do not release debris particles.

Following the manufacturing, cleaning, inspection, and assembly processes, it would be ideal to perform hot-fire tests of future systems. If a full-system hot-fire test is infeasible, FlatSat tests should utilize flight-identical components whenever possible. The LFPS design was hot-fire tested in a FlatSat configuration with many flight-like components, but this testing did not utilize a flight-like tank or manifold. Hot-fire testing with a 3D-printed manifold featuring similar geometry and orifices might have identified the FOD issue on the ground, especially if the component underwent vibration testing prior to hot-fire testing. While an abridged flow test

was performed on the flight manifold after environmental testing, it utilized helium, which would not have been sufficient to indicate FOD-restricted flow.

System Capabilities

The designed capabilities of the LFPS were sufficient for executing a nominal mission. However, operating in an anomalous state uncovered certain system limitations. For example, while the LFPS controller was designed to process at least five commands per second, the spacecraft C&DH architecture ended up limiting propulsion commands originating from FSW to one every two seconds. This severely limited certain types of manual operations. If this limitation had been better understood, more efficient commands could have been implemented, such as a single command which would fire each thruster at specified duty cycles for two seconds, allowing for continuous manual pulsing of all thrusters.

The reduced performance anomaly led to unplanned use of single thrusters at varied temperatures and duty cycles. The fact that only one valve was instrumented with a thermocouple meant that temperatures of other valves had to be inferred by models developed from the single-valve data. This data was especially limited since the telemetered valve was associated with thruster 1, which never performed nominally during flight. Including temperature feedback on all valves would have allowed for longer maneuvers without having to rely on the safety margin of the time-based thermal models.

CONCLUSION

The Lunar Flashlight Propulsion System successfully demonstrated the ASCENT monopropellant technology, producing about 16.2 m/s of delta-v and reducing spacecraft momentum during various parts of the mission. However, the variable performance of this system made clear that additional precautions must be taken during the design and manufacturing of future propulsion systems in this family. Most importantly, even with more robust cleanliness and internal surface finishing standards, integrated propellant filters are critical for preventing particles from collecting in the tight orifices of these small systems. Also, additional ground testing, including random vibration environmental tests followed by thruster hot-fire tests, could allow for identification and resolution of FOD-related issues prior to launch. Although many of these risk-reducing concepts were brought up in preflight reviews, the extremely tight development timeline prevented their execution.

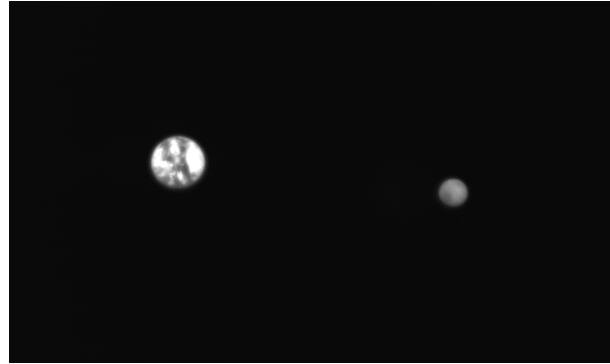


Figure 24: Image of Earth (Left) and Moon (Right) Captured by Lunar Flashlight on March 23, 2023

Lunar Flashlight was overall a successful technology demonstration of the LFPS and multiple other subsystems, and as of this writing, the spacecraft continues to operate in a heliocentric orbit. The science payload performed better than expected, with a higher detector signal-to-noise ratio than seen in ground testing. Laser stress tests demonstrated the instrument's ability to perform 90-second experiments in the space environment, along with over 793 seconds of tightly scheduled autonomous experiments which illuminated multiple Earth and space-based observatories during the single Earth perigee. Thermal data proved that the instrument radiator could passively cool the detector to below -60°C . These results indicated that the science mission could have been successfully performed if the spacecraft had encountered the Moon at an appropriate distance. The XACT-50, serving as the mission's ACS, performed as expected, and exceeded the team's expectations during more complicated activities such as the rotating TCMs. It was also used to capture Earth and Moon images (Figure 24). The power subsystem, including solar arrays, EPS, and batteries, exceeded prelaunch analyses, providing the system with plenty of power margin during all activities including off-sun thrusting and Earth eclipse. The C&DH and FSW also performed as expected, allowing the team to reliably control the spacecraft, and even demonstrating an in-flight FSW update. Finally, the Iris radio also exceeded expectations, operating continuously in full-duplex mode for over 80 hours without exceeding thermal limits, and acting as the first in-flight demonstration of Pseudorandom-Noise (PN) Delta Differential One-way Ranging (DDOR) with NASA's Deep Space Network. The knowledge gained from the development and operation of this spacecraft and its propulsion system provides a set of important lessons for future CubeSat propulsion systems and missions.

ACKNOWLEDGEMENTS

A portion of this research was carried out at the Jet Propulsion Laboratory, California Institute of Technology, under NASA contract 80NM0018D0004.

The propulsion team was strengthened by the help from these individuals: Christopher Bostwick, Daniel Cavender, Carlos Diaz, Mackenzie Kilcoin, Shawn Skinner, Nehemiah Williams, and Hunter Williams.

The MDNav team enabled new ways of keeping LF on track to reach the Moon throughout the propulsion system anomaly: Stefano Campagnola, Andrew Cox, Stuart Demcak, Eric Graat, Eric Gustafson, Jennie Johannesen, Julie Kangas, Gregory Lantoine, Jules Lee, Timothy (Tim) McElrath, Sumita Nandi, Mark Ryne, and Theodore Sweetser. Tim led the development of the rotating TCM, helping to mature it from concept to reality. Stuart performed a lead role on the navigation team and processed data plotted in this paper.

The FSW team of two, Kevin Ortega and Aadil Rizvi, enabled new functionality that allowed a wider range of propulsion system activities to be performed safely.

Steven (Steve) Collins, Kevin Lo, and David Sternberg provided ACS support, ultimately allowing for more complicated maneuvers such as the rotating TCM to be performed. Steve proposed the rotating TCM idea. Michael Hauge, Graham Jordan, and Shan Selvamurugan from GT also stepped up to provide essential ACS support.

Mission Management and Mission Assurance roles were filled by Andrew Klesh, Christina Kneis, Jack Trinh, and Bruce Waggoner, where they promoted mission success by applying appropriate planning and risk management strategies.

Finally, the Georgia Tech mission operations team made each flight activity possible with their unwavering support at all hours of the day and night. Special appreciation goes to Michael Hauge and Mason Starr for their lead roles during these activities. Also, Conner Awald, Marilyn Braojos, John Cancio, Graham Jordan, Robert Lammens, and Shan Selvamurugan are recognized for their roles as activity leads and mission planners. Additional operations team members who made this possible include Katherine Anderson, Shalomi Arulpragasam, Kieran Barket, Emma Hanson, Mollie Johnson, Evan Leleux, Bryn Merrell, Micah Pledger, Katy Ryan, Cate Schlabach, Andrew Weatherly, and Alan Yeung. Jud Ready is acknowledged for his support at Georgia Tech during SI&T, fueling, and operations.

REFERENCES

- [1] D. Andrews, G. Huggins, E. G. Lightsey, N. Cheek, N. Daniel, A. Talaksi, S. Peet, L. Littleton, S. Patel, L. Skidmore, M. Glaser, D. Cavender, H. Williams, D. McQueen, J. Baker, and M. Kowalkowski, "Design of a Green Monopropellant Propulsion System for the Lunar Flashlight CubeSat Mission," in *Proceedings of the Small Satellite Conference*, 2020.
- [2] B. A. Cohen, P. O. Hayne, B. Greenhagen, D. A. Paige, C. Seybold, and J. Baker, "Lunar Flashlight: Illuminating the Lunar South Pole," *IEEE Aerospace and Electronic Systems Magazine*, vol. 35, no. 3, pp. 46–52, 2020.
- [3] B. A. Cohen, P. O. Hayne, C. G. Paine, D. A. Paige, and B. T. Greenhagen, "Lunar Flashlight: Mapping Lunar Surface Volatiles Using a CubeSat," in *46th Lunar and Planetary Science Conference*, 2015.
- [4] C. Smith, D. Cavender, L. Littleton, and E. G. Lightsey, "Assembly Integration and Test of the Lunar Flashlight Propulsion System," in *AIAA SciTech 2022 Forum*, 2022.
- [5] L. M. Littleton and E. G. Lightsey, "Assembly, Integration, and Testing of a Green Monopropellant Propulsion System for NASA's Lunar Flashlight Mission," 2021.
- [6] N. Cheek, N. Daniel, E. G. Lightsey, S. Peet, C. Smith, and D. Cavender, "Development of a COTS-Based Propulsion System Controller for NASA's Lunar Flashlight CubeSat Mission," in *Proceedings of the Small Satellite Conference*, 2021.
- [7] N. Cheek, C. Gonzalez, P. Adell, J. Baker, C. Ryan, S. Statham, E. G. Lightsey, C. Smith, C. Awald, and J. Ready, "Systems Integration and Test of the Lunar Flashlight Spacecraft," in *Proceedings of the Small Satellite Conference*, 2022.
- [8] T. P. McElrath, S. Collins, and C. Smith, "A Delicate Balance of Torque and Thrust: How Lunar Flashlight Used Rotating Maneuvers to Make One Thruster Do the Work of Four," in *AIAA/AAS Astrodynamics Specialist Conference*, to be published.
- [9] M. Starr, "Development of Tactical and Strategic Operations Software for NASA's Lunar Flashlight Mission," in *Proceedings of the Small Satellite Conference*, 2023.